

# A GENERALIZED MATHEMATICAL MODEL FOR EFFICIENCY CALIBRATION OF GAMMA DETECTORS

## Application to Practical Cases

by

**Nikola N. MIHALJEVIĆ**<sup>1,2</sup>, **Slobodan I. JOVANOVIĆ**<sup>2,3\*</sup>, and **Aleksandar D. DLABAC**<sup>2</sup>

<sup>1</sup>Department of Mathematics, Maritime Faculty, University of Montenegro, Kotor, Montenegro

<sup>2</sup>Centre for Nuclear Competence and Knowledge Management, University of Montenegro, Podgorica, Montenegro

<sup>3</sup>Department of Physics, Faculty of Natural Sciences and Mathematics, University of Montenegro, Podgorica, Montenegro

Scientific paper

<https://doi.org/10.2298/NTRP181031006M>

Efficiency calibration, *i. e.* determination of detection efficiency,  $\varepsilon_p$ , is a crucial issue in gamma spectrometry (quantification of gamma spectroscopic measurements) with semiconductor and scintillation detectors. Comparing three possible ways to addressing the problem – relative, absolute and semi empirical – advantages of the latter are emphasized. Among semi empirical models, efficiency transfer using effective solid angles,  $\bar{\Omega}$ , is sorted out and briefly elaborated. This approach reduces the problem of efficiency calibration to the determination of  $\bar{\Omega}$ . It proved reliable and has been broadly used in practice, mainly in the form of the long existing ANGLE software. Progressing further, a generalized mathematical formula for calculations is developed – first of the kind – offering an opportunity for advanced applications of gamma spectrometry. The formula enables unlimited flexibility in application, as it conveniently separates the source data from the detector data during the integration procedures ( $\bar{\Omega}$  calculations). Its practicality is demonstrated for a number of typically encountered counting arrangements, as well as for some exotic ones. The relevant formulae are used in PC calculations and numerical testing is further performed so as to check the validity of the mathematical method and the computer code. Care was taken of the optimization of complex numerical procedures employed (involving fivefold numerical integration), so as to keep computation times as low as possible (in order of minutes or even seconds on ordinary PC). Results obtained are affirmative for both the method and the code. The model will be gradually incorporated into ANGLE software, thus making it readily available for routine use by gamma spectrometry community.

*Key words:* gamma spectrometry, detection efficiency, detector calibration, mathematical model, numerical testing, applicability, ANGLE software

## INTRODUCTION

Forty years have passed since the advent of semiconductor detectors and their subsequent introduction into analytical practice, and even seventy from the scintillation ones; quantification of gamma spectroscopic measurements is still a challenging task, for which no definite/general practical solution is available so far. Given the fact gamma spectroscopy is one of the two most widely applied techniques in nuclear sciences, applications and industry (the other one being radiation dosimetry), that speaks on its own about the importance of the topic.

For clarity purposes let us first distinguish *spectroscopy* as qualitative, and *spectrometry* as quantitative analysis of gamma and/or X-ray emitting (*i. e.*

spectroscopic) samples/sources. Here *qualitative* means determining which radionuclides are present in the sample and *quantitative* in what quantities (*i. e.* concentrations) they are present. In other words, spectrometry means quantification of spectroscopic measurements. Unfortunately, these two terms are often indiscriminately/exchangeably used in literature, which may confuse the reader, especially a newcomer to the field.

A gamma spectrum is collected during a spectroscopic measurement (counting) by a gamma spectroscopic system, which basically consists of a detector, coupled with multi channel analyzer, and supporting electronics. Here the term *detector* encompasses mainly semiconductor and scintillation ones, as the vast majority of gamma detectors in use nowadays belong to these two categories.

\* Corresponding author; e-mail: bobo\_jovanovic@yahoo.co.uk

Spectrum here represents a distribution of registered photon interactions (within the detector active body) vs. photon energy. Radionuclides are easily distinguished by their characteristic (fingerprint) spectra of gamma and X-rays, enabling nuclide identification from readily available nuclear data libraries. Spectroscopic analysis is thus reduced to energy calibration of the system/detector used, which is a pretty simple, even trivial task.

Spectrometric analysis is about converting the number of counts (collected in full energy peaks in the spectrum) into the activities of the corresponding radionuclide(s) present in the sample (source). Spectrometry basically goes about efficiency calibration for the given counting arrangement (counting arrangement being the ensemble of the detector, source with its container, and all gamma intercepting/absorbing layers in between). Efficiency calibration can be simple in some particular cases (*e. g.* due to symmetry of the counting arrangement), but in principle it is not – in fact on the contrary, it is a complex problem, for which no general solution has been provided up to now; *see e. g.* classic radiation detection textbooks [13]. Huge and ever growing evidence in scientific papers are testimony to the efforts being continuously paid to this aim by the gamma spectrometric community.

There are, in principle, three approaches to efficiency calibration of semiconductor and scintillation detectors [4]:

(1) *Relative*, where one tries to imitate as much as possible the source by a standard (or *vice versa*) while keeping the same counting conditions for the two. Paid enough care, the result is, in general, so accurate that cannot be surpassed by other methods. However, gamma spectrometrists know too well what *enough care* means in practice. Combined with the utmost inflexibility in respect with varying source and container parameters (shape, dimensions, material composition, positioning), this represents *raison d'être* of the other approaches, which follow.

(2) *Absolute* calculations are purely mathematical approaches, with no supporting experimental evidence whatsoever for the detector response. These are usually variations of Monte Carlo (MC) methods. The MC are essentially statistical treatments of the events which photons undergo – from being emitted by a source atom until the interaction with the detector active body – including the treatment of the so produced electrons, positrons and other subsequent energy carriers.

The absolute approach is beautifully exact, with the condition that we consider a sufficiently large number of incident photons, and that we know the details about (1) source, detector and intercepting layers' geometrical/compositional data, (2) the corresponding photon attenuation coefficients, (3) energy and angle dependent cross sections for various photon interactions with the detector active body, and (4) parameters characterizing electron/positron behavior in the latter.

In principle, unsatisfactory manufacturers' detector specifications and relatively poor knowledge of (many of) the previous physical parameters turn out to be the limiting factors for its applicability. Inherent statistical uncertainty of MC methods is a drawback as well. However, with ever speeding up of computers, and with more accurate detector specifications and cross-section data (the determination of which is, on its turn, related to more careful and sophisticated measurements), it is reasonable to assume that time works for absolute methods, and that in future they might become the dominant ones.

(3) *Semi empirical* models, trying to conciliate the previous two. Semi empirical models commonly consist of two parts: (1) experimental, producing one kind or another of reference efficiency characteristic of the detector (detector response) and (2) relative to this calculation of  $\varepsilon_p$ . The inflexibility of the relative method is avoided this way, as well as the demand for some physical parameters needed in absolute calculations.

Numerous variations exist within semi empirical approach, with emphases either on experimental or on calculation/computational part. However, most of these simplify (or oversimplify) the physical model behind, *i. e.* the treatment of (1) gamma attenuation, (2) counting geometry, and (3) detector response. Moens *et al.* [5] showed that only the simultaneous differential treatment of these three factors is essentially justified – any simplification would mean that the exactness of the approach would be compromised. This fact is transformed into the concept of the effective solid angle,  $\bar{\Omega}$ , a calculated value incorporating the three components, and closely/simplely related to detection efficiency (see further) – by determining  $\bar{\Omega}$  one practically determines  $\varepsilon_p$ . Calculation of effective solid angles can, therefore, be considered as the key to quantitative gamma spectrometry.

A few hundred thousand gamma spectrometric systems are in operation nowadays worldwide. The majority of these are used for spectroscopic purposes (*i. e.* qualitative analyses) only; the remainder is used for spectrometry (quantification) as well. Among the latter, the relative approach is still the most exploited one, perhaps just because of the inertia in work. With due respect for the quality of results obtained by the relative method, this is a deplorable fact: by relying exclusively on relative method, expensive equipment in the labs and precious human resources are used far below their potential.

## THEORETICAL

### The effective solid angle and efficiency transfer

Given a gamma source (S) and a gamma detector (D), fig. 1, the effective solid angle is defined as [46]

$$\bar{\Omega}_{S_D} = d\bar{\Omega}, \text{ with } d\bar{\Omega} = \frac{F_{\text{att}} F_{\text{eff}} TP \vec{n}}{|TP|^3} d\sigma \quad (1)$$

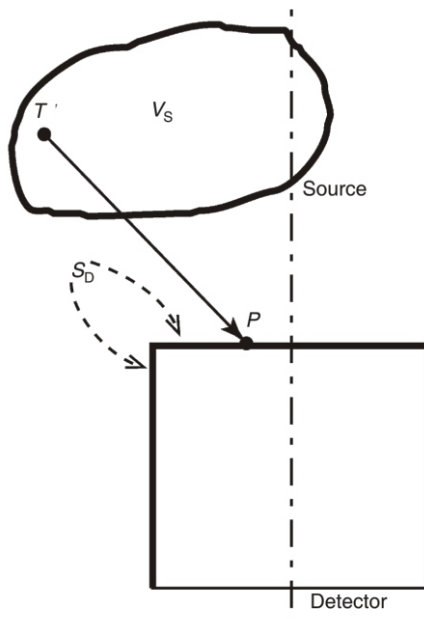


**Figure 1.** To the definition of the effective solid angle,  $\bar{\Omega}$ , eq. (1); thick line represents the detector surface  $S_D$  visible by the source

where  $V_S$  is the source volume and  $S_D$  = detector surface exposed to the source (*visible* by the source).

Here  $T$  is point varying over  $V_S$ ,  $P$  point varying over  $S_D$ , and  $\vec{n}$  the external unit vector normal to infinitesimal area  $d\sigma$  at  $S_D$ . Equation (1) is thus a fivefold integral. Factor  $F_{att}$  accounts for gamma attenuation of the photon following the direction  $TP$  out of the detector active zone, while  $F_{att}$  describes the probability of an energy degradable photon interaction with the detector crystal (*i. e.* coherent scattering excluded), initiating the detector response. The two factors include therefore geometrical and compositional parameters of the materials traversed by the photon.

With  $\varepsilon_p$  being proportional to  $\bar{\Omega}$  the detection efficiency is found as

$$\varepsilon_p = \varepsilon_{p,ref} \frac{\bar{\Omega}}{\bar{\Omega}_{ref}} \quad (2)$$

where index ref denotes reference counting geometry to which the actual one is relative. This is basically the efficiency transfer [7-10] using effective solid angles; it can thus be addressed as ET- $\bar{\Omega}$  method for detection efficiency calibration/determination.

Note that the above  $\varepsilon_p$  vs.  $\bar{\Omega}$  proportionality holds under the condition that peak to total ratio ( $P/T$ ) is an intrinsic characteristic of the actual detector – fairly constant and dependent on gamma energy only. This is generally assumed to be the case [5, 11-15], but caution is called upon not to exaggerate/overreach with its applicability, especially with low gamma/X-ray energies and extended geometries. From the other side, attempting exact treatment of  $P/T$  variations for a given detector and varying counting conditions would hugely complicate the (already complex) detection efficiency issue. Apparently, the key words here are *trade off* and *practi-*

*cality*: for most gamma spectrometry applications, a few percent uncertainties in  $\varepsilon_p$  are acceptable and perceived as a realistic expectation; it should be further stressed that  $P/T$  usually contributes only a small fraction of that. In environmental radioactivity monitoring, for instance, the acceptable uncertainties are 5-10 %, in waste management and nuclear decommissioning 10-20 % and in some application even higher. A notable exception is radiation metrology, where uncertainties even below 1 % may be requested – a condition only relative method could realistically meet/comply with.

So as to apply the ET- $\bar{\Omega}$  method the following should be known:

- *reference efficiency curve*, obtained by counting some known (calibrated) source(s) at a reference position, and covering gamma energies,  $E_\gamma$  in the region of interest (*e. g.* 50-3000 keV); considerable effort/care should be paid in this phase to reach accurate  $\varepsilon_{p,ref}$  vs.  $E_\gamma$  function, but it largely pays off in further exploitation;
- *geometrical and compositional data* about the source, detector and all intercepting layers (the latter including source container and holder, detector end cap and housing, crystal dead layers, etc.); and
- *gamma attenuation coefficients and densities* for all materials involved.

The method was originally introduced for the use in neutron activation analysis ( $k_0$ -NAA) and was limited to the simple case of cylindrical sources coaxially positioned with the detector, and with radii smaller than that of the detector [5].

### Application in ANGLE software

Following the experiences with post Chernobyl (1986) monitoring of radioactivity in various types of bulky samples, the method was initially expanded to large cylindrical sources [16] and Marinelli type ones [17]. The first version of ANGLE software, with its characteristic user friendly graphical interface, appeared in 1994; it was written for DOS operating system and supported various HPGe and Ge(Li) detectors (coaxial, planar, well type) [4]. The enthusiastic/affirmative acceptance and constructive feedback by the spectrometric community has inspired work on the code development to continue ever since, producing numerous updates/upgrades.

The latest version ANGLE 4 [18] was released in 2016, fully refurbished and introducing many new functionalities, including (1) support to scintillation detectors (in addition to the existing semiconductor ones), (2) *discrete* reference characterization of the detector, (3) XML file format, (4) command line parameters, (5) scaled preview (with zooming option) of the counting arrangement, including all relevant details: detector, source, container, intercepting layers, and

their positioning, (6) multilanguage support (currently operating in English, Chinese, Russian, French, Japanese and Spanish), etc.

In its various versions, ANGLE is nowadays in use in hundreds of gamma spectrometry based analytical laboratories worldwide (ref. [18]).

### Mathematical generalization

Apparently, a generalization of the formula (1) into a form which can be readily applicable to any practical counting arrangement (source, detector, geometry) is not an easy mathematical task. The issue was tackled by quite a number of authors, however with solutions bound with more or less restraining conditions. The complexity, yet reliability of the theoretical approach, followed by numerical calculations is even more prominent in some other areas of gamma spectrometry [19]. Our approach to generalization is one of the unlimited flexibilities, based on simple structuring of integration intervals – over the source volume (threefold integration) and over the detector visible surface (twofold integration), separating the source from the detector in the integration process, as follows.

Starting with a point source arbitrarily positioned vs. a cylindrical detector [20], fig. 2, we obtain

$$\bar{\Omega} = \int_{\theta_1}^{\theta_0} \int_{R_0}^{R_0} F_{att} F_{eff} \bar{F}_1(T, P_{S_1}) R dR d\theta + \int_{\theta_0}^{\theta_0} \int_{R_0}^H F_{att} F_{eff} \bar{F}_2(T, P_{S_2}) dh + \int_{\theta_0}^{\theta_0} \int_{R_0}^{R_0} F_{att} F_{eff} \bar{F}_4(T, P_{S_4}) R dR d\theta \quad (3)$$

where  $S_D = S_1 + S_2 + S_3 + S_4$ . For a true cylindrical detector, with no edge rounding (bulletization),  $S_3 =$  thus:  $S_D = S_1 + S_2 + S_4$  [20].

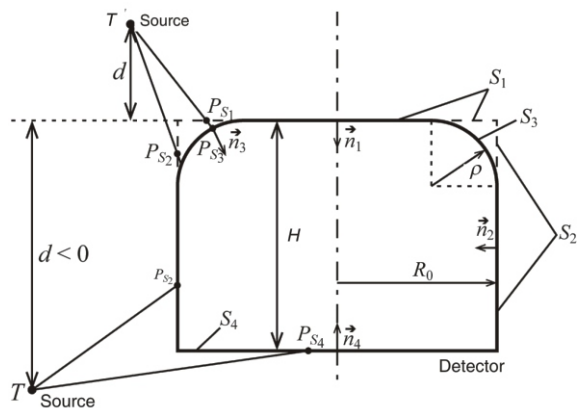


Figure 2. Point source arbitrarily positioned vs. the detector

Note that the above  $\bar{\Omega}$  value for point source, eq. (3), will feature as sub integral function in all subsequent formulae for complex sources, whereby integration over the source volume will be additionally performed, without combining them within an integrand; this is critical for generalization.

The co-ordinate system is positioned as illustrated in figs. (4-7). Since for *bulletized* detectors parts of surfaces  $S_1$  and  $S_2$  are virtual (dashed lines in fig. 2), functions  $\bar{F}_1$  and  $\bar{F}_2$  can be expressed as

$$\bar{F}_1(T, P_{S_1}) = \frac{TP_{S_1} \bar{n}_1}{|TP_{S_1}|^3}, z_r \quad 0 \quad RR_0 \quad \rho$$

$$\bar{F}_2(T, P_{S_2}) = \frac{TP_{S_2} \bar{n}_2}{|TP_{S_2}|^3}, x_T^2 \quad y_T^2 \quad R_0^2 \quad h \quad \rho$$

$$\bar{F}_3(T, P_{S_3}) = \frac{TP_{S_3} \bar{n}_3}{|TP_{S_3}|^3}, z_T \quad 0 \quad R \quad R_0 \quad \rho \quad TP_{S_1} \quad S_3$$

$$\bar{F}_4(T, P_{S_4}) = \frac{TP_{S_4} \bar{n}_4}{|TP_{S_4}|^3}, z_T \quad H \quad R \quad R_\rho$$

$$\bar{F}_5(T, P_{S_5}) = \frac{TP_{S_5} \bar{n}_5}{|TP_{S_5}|^3}, z_T \quad H \quad R \quad R_\rho$$

$$0, z_T \quad 0 \quad R \quad R_0 \quad \rho \quad TP_{S_1} \quad S_3$$

$$0, z_T \quad 0$$
(4)

with  $P_{S_1} (R \cos \theta, R \sin \theta, 0), \bar{n}_1 (0, 0, 1), R [0, R_0], \theta [0, 2\pi], P_{S_2} (R_0 \cos \theta, R_0 \sin \theta, h), \bar{n}_2 (\cos \theta, \sin \theta, 0), P_{S_3} (R_0, 0, 0), \bar{n}_3 (1, 0, 0), P_{S_4} (R_0, 0, H), \bar{n}_4 (0, 0, 1), P_{S_5} (R_0, 0, 0), \bar{n}_5 (1, 0, 0)$  [20]

$$\bar{F}_1(T, P_{S_1}) = \frac{TP_{S_1} \bar{n}_1}{|TP_{S_1}|^3}, z_r \quad 0 \quad RR_0 \quad \rho$$

$$\bar{F}_2(T, P_{S_2}) = \frac{TP_{S_2} \bar{n}_2}{|TP_{S_2}|^3}, x_T^2 \quad y_T^2 \quad R_0^2 \quad h \quad \rho$$

$$\bar{F}_3(T, P_{S_3}) = \frac{TP_{S_3} \bar{n}_3}{|TP_{S_3}|^3}, z_T \quad 0 \quad R \quad R_0 \quad \rho \quad TP_{S_1} \quad S_3$$

$$\bar{F}_4(T, P_{S_4}) = \frac{TP_{S_4} \bar{n}_4}{|TP_{S_4}|^3}, z_T \quad H \quad R \quad R_\rho$$

$$\bar{F}_5(T, P_{S_5}) = \frac{TP_{S_5} \bar{n}_5}{|TP_{S_5}|^3}, z_T \quad H \quad R \quad R_\rho$$

$$0, x_T^2 \quad y_T^2 \quad R_0^2 \quad h \quad \rho \quad TP_{S_2} \quad S_3$$

$$0, x_T^2 \quad y_T^2 \quad R_0^2$$
(5)

with  $P_{S_2} (R_0 \cos \theta, R_0 \sin \theta, h), \theta [\theta_0, \theta_1], h [H, 0], \bar{n}_2 (\cos \theta, \sin \theta, 0), P_{S_3} (R_0, 0, 0), \bar{n}_3 (1, 0, 0), P_{S_4} (R_0, 0, H), \bar{n}_4 (0, 0, 1), P_{S_5} (R_0, 0, 0), \bar{n}_5 (1, 0, 0)$

$$\bar{F}_1(T, P_{S_1}) = \frac{TP_{S_1} \bar{n}_1}{|TP_{S_1}|^3}, z_r \quad 0 \quad RR_0 \quad \rho$$

$$\bar{F}_2(T, P_{S_2}) = \frac{TP_{S_2} \bar{n}_2}{|TP_{S_2}|^3}, x_T^2 \quad y_T^2 \quad R_0^2 \quad h \quad \rho$$

$$\bar{F}_3(T, P_{S_3}) = \frac{TP_{S_3} \bar{n}_3}{|TP_{S_3}|^3}, z_T \quad 0 \quad R \quad R_0 \quad \rho \quad TP_{S_1} \quad S_3$$

$$\bar{F}_4(T, P_{S_4}) = \frac{TP_{S_4} \bar{n}_4}{|TP_{S_4}|^3}, z_T \quad H \quad R \quad R_\rho$$

$$\bar{F}_5(T, P_{S_5}) = \frac{TP_{S_5} \bar{n}_5}{|TP_{S_5}|^3}, z_T \quad H \quad R \quad R_\rho$$

$$0, z_T \quad H$$
(6)

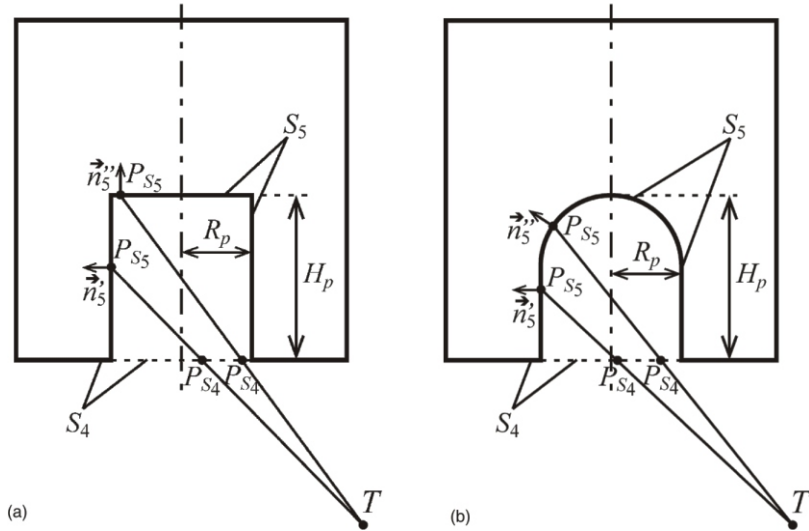


Figure 3. Two possible configurations of the detector contact cavity; flat (a) and rounded (b)

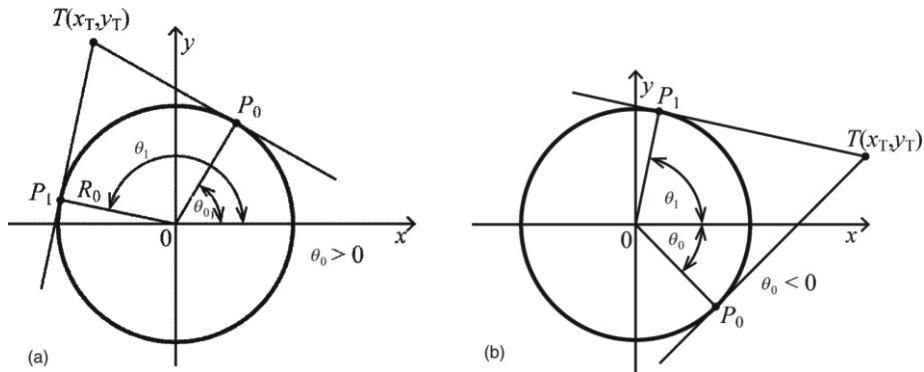


Figure 4. Integration limits for the angle  $\theta$ :  $\theta_0 > 0$  (a),  $\theta_0 < 0$  (b)

where  $P_{S_4}(R \cos \theta, R \sin \theta, H)$ ,  $R \in [0, R_0]$ ,  $\theta \in [0, 2\pi]$ ,  $\vec{n}_4(0, 0, 1)$ ,  $P_{S_5} TP_{S_4} S_5$ , and  $\vec{n}_5 = \vec{n}_5(P_{S_5})$ ; the latter comes to either:

$$\vec{n}_5' = \vec{n}_5'' = \vec{n}_5''', \text{ with } \vec{n}_5' = (x_5, y_5, 0) / \sqrt{x_5^2 + y_5^2},$$

$$\vec{n}_5'' = (0, 0, 1) \text{ for flat contact cavity, fig. 3(a), or}$$

$$\vec{n}_5''' = (x_5, y_5, z_5 - D_p - R_p) / \sqrt{x_5^2 + y_5^2 + (z_5 - D_p - R_p)^2}$$

for rounded contact cavity, fig. 3(b), where  $x_5, y_5, z_5$  are the co-ordinates of  $P_{S_5}$  and  $D_p = H - H_p$ ; note that in fig. 3 proportions of the cavity are distorted for visual clarity.

Angles  $\theta_0$  and  $\theta_1$ , fig. 4 are obtained as

$$\theta_{0,1} = \begin{cases} \arccos \hat{x}_{0,1}, & \hat{y}_{0,1} \geq 0 \\ 2\pi - \arccos \hat{x}_{0,1}, & \hat{y}_{0,1} < 0 \end{cases}$$

with

$$\hat{x}_{1,0} = \frac{R_0 |x_T|}{x_T^2 + y_T^2} \sqrt{x_T^2 + y_T^2 + R_0^2} \operatorname{sgn} x_T$$

$$\hat{y}_{0,1} = \frac{R_0 y_T}{x_T^2 + y_T^2} \sqrt{x_T^2 + y_T^2 + R_0^2}$$

If  $x_T = 0$  (point at  $y$ -axis), then:

$$\hat{y}_0 = \hat{y}_1 = \frac{R_0^2}{y_T} \text{ and } \hat{x}_{1,0} = \frac{\sqrt{R_0^2 + \hat{y}_{0,1}^2}}{R_0}$$

By defining sub integral functions  $\bar{F}_1, \bar{F}_2$ , and  $\bar{F}_4$  in the previous manner, integration limits for the source are becoming independent of the detector dimensions, as well as of the source positioning vs. the detector. Note this was previously not the case [6] – integration over the detector surface  $\int_{R_0}^r r dr$  was rather inseparable from the integration over the source volume, which was a limiting factor for applicability.

Thus, integration limits over the source are now independent of the detector whatsoever. This *disconnection*, i. e. source detector separation in the integration process is a novelty in mathematical modelling of efficiency calculations. Apparently, it has a crucial consequence in enabling unlimited flexibility and hence generalization of the model.

As to geometry, source position vs. the detector is defined by the coordinates of the point  $T(x_0 + \dots, y_0 + \dots, d + \dots)$ , where  $x_0, y_0$  are the source axial displacements (shifts) from the detector in horizontal ( $Oxy$ ) plane and  $d$  is vertical distance between the source bottom surface and the detector upper surface ( $S_1$ ). It can

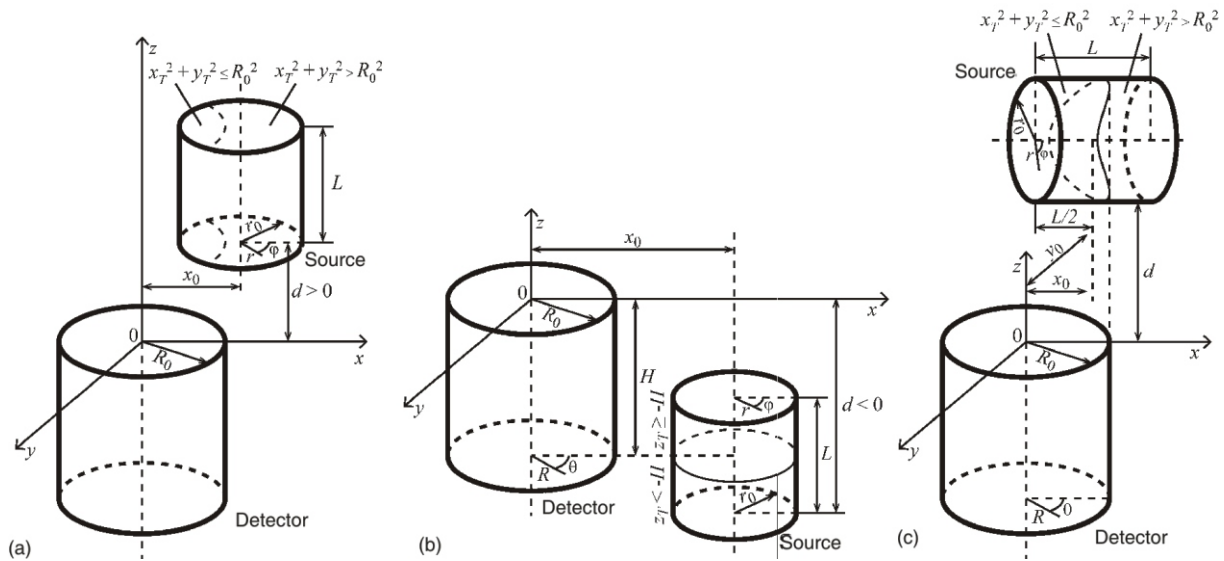


**Figure 5.** Cylindrical source positioned above the detector with parallel axes (a), by the detector side with parallel axes (b), and above the detector with perpendicular axes (c)

be positive or negative, depending on whether the source bottom surface is above  $S_1$  or below it.

**Application to some specific source shapes**

Equation (3) can readily be applied to most situations encountered in gamma spectrometry practice. Few examples concerning most common source vs. detector positioning, as well as some not so common, are given below.

*Cylindrical sources*

For a cylindrical source coaxial with the detector, figs. 5(a), and 5(b), eq. (3) gives

$$\bar{\Omega} = \frac{1}{r_0^2 L \pi} \int_0^L \int_0^{2\pi} \int_0^{r_0} \int_0^{2\pi} \int_0^{R_0} F_{att} F_{eff} \bar{F}_1(T, P_{S_1}) R dR d\theta_0 d\theta_1 r dr d\varphi_0 d\varphi_1 \quad (7)$$

with  $T(x_0 + r \cos\varphi, r \sin\varphi, d + l)$  and  $x_0$  axial displacement of the source vs. the detector.

For a perpendicularly positioned cylindrical source, fig. 5(c) we obtain

$$\bar{\Omega} = \frac{1}{r_0^2 L \pi} \int_{-\frac{L}{2}}^{\frac{L}{2}} \int_0^{2\pi} \int_0^{r_0} \int_0^{2\pi} \int_0^{R_0} F_{att} F_{eff} \bar{F}_1(T, P_{S_1}) R dR d\theta_0 d\theta_1 r dr d\varphi_0 d\varphi_1 \quad (8)$$

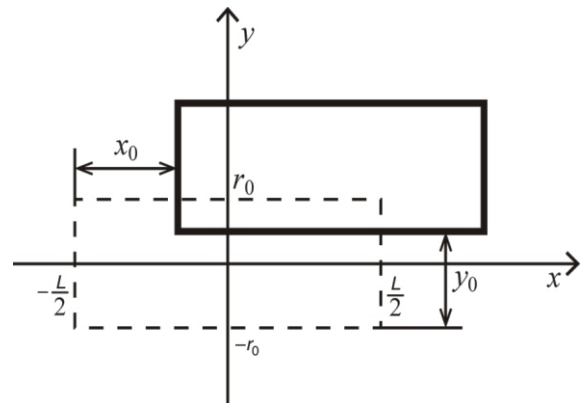


**Figure 6.** Horizontal axial displacement (in  $Oxy$  plane) of a perpendicularly positioned cylindrical source vs. the detector, fig. 5(c)

with  $T(x_0 + l, y_0 + r \sin\varphi, d + r_0 + r \cos\varphi)$  and  $x_0, y_0$  horizontal axial displacements (in  $Oxy$  plane) of the source vs. the detector, fig. 6.

*Marinelli sources*

For Marinelli type sources, fig. 7, eq. (3) yields

$$\bar{\Omega} = \frac{1}{W} \int_0^L \int_0^{2\pi} \int_0^{r_0} \int_0^{2\pi} \int_0^{R_0} F_{att} F_{eff} \bar{F}_1(T, P_{S_1}) R dR d\theta_0 d\theta_1 r dr d\varphi_0 d\varphi_1 \quad (9)$$

with  $T(x_0 + r \cos\varphi, r \sin\varphi, d + l)$ ,  $x_0$  axial displacement of the source vs. the detector, and

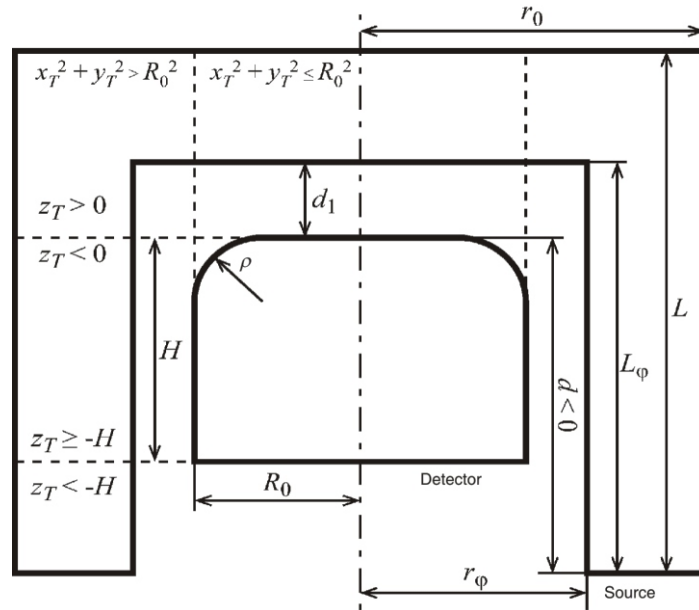


Figure 7. Marinelli type source

$$W = \begin{matrix} d & d_1 & L_\phi \\ r_1(l) & 0, l & L_\phi \\ & r_\phi & l & L_\phi \\ & (r_0^2 L & r_\phi^2 L_\phi) \pi, & L & L_\phi \\ & (r_0^2 & r_\phi^2) L \pi, & L & L_\phi \end{matrix}$$

Spherical sources

For a spherical source, fig. 8, we obtain

$$\bar{\Omega} = \frac{3}{4r_0^3} \int_0^\pi \int_0^{2\pi} \int_0^{R_0} \sin\psi d\psi d\varphi r^2 dr \int_0^H F_{att} F_{eff} \bar{F}_1(T, P_{S_1}) R dR + \int_0^H \int_0^{2\pi} \int_0^{R_0} \sin\psi d\psi d\varphi r^2 dr \int_0^H F_{att} F_{eff} \bar{F}_2(T, P_{S_2}) dh + \int_0^H \int_0^{2\pi} \int_0^{R_0} \sin\psi d\psi d\varphi r^2 dr \int_0^H F_{att} F_{eff} \bar{F}_4(T, P_{S_4}) R dR \quad (10)$$

with  $T(x_0 + r \sin\psi \cos\varphi, r \sin\psi \sin\varphi, d + r_0 + r \cos\psi)$  and  $x_0$  displacement of the center of the sphere from the detector axis; various possibilities of positioning are illustrated in fig. 9.

Cuboid sources

For cuboid (rectangular parallelepiped) type sources, fig. 10, we obtain

$$\bar{\Omega} = \frac{1}{abL} \int_0^L \int_0^a \int_0^b \int_0^{2\pi} \int_0^{R_0} \sin\psi d\psi d\varphi r^2 dr \int_0^H F_{att} F_{eff} \bar{F}_1(T, P_{S_1}) R dR + \int_0^H \int_0^{2\pi} \int_0^{R_0} \sin\psi d\psi d\varphi r^2 dr \int_0^H F_{att} F_{eff} \bar{F}_2(T, P_{S_2}) dh + \int_0^H \int_0^{2\pi} \int_0^{R_0} \sin\psi d\psi d\varphi r^2 dr \int_0^H F_{att} F_{eff} \bar{F}_4(T, P_{S_4}) R dR \quad (11)$$

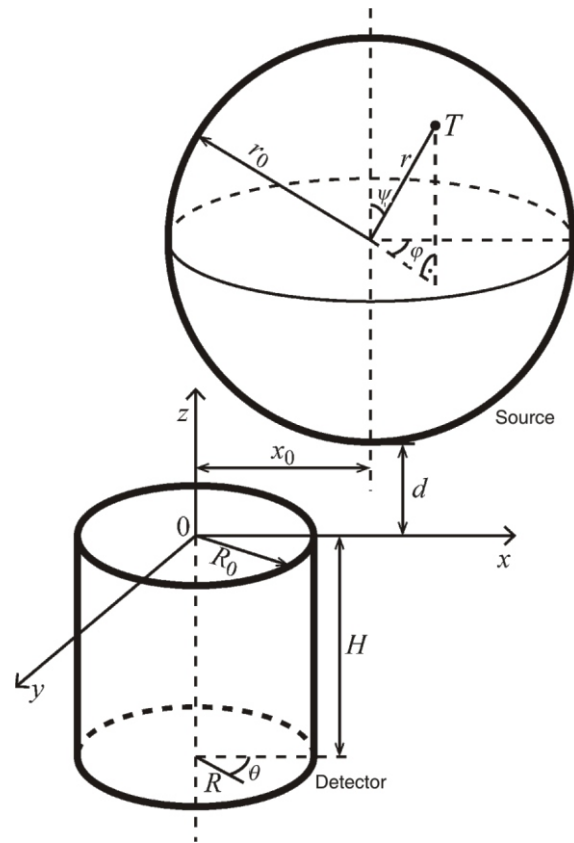


Figure 8. Spherical source

with  $T(x_0 + x, y_0 + y, d + 1)$  and  $x_0, y_0$  horizontal axial displacements (in Oxy plane) of the source vs. the detector, fig. 11.

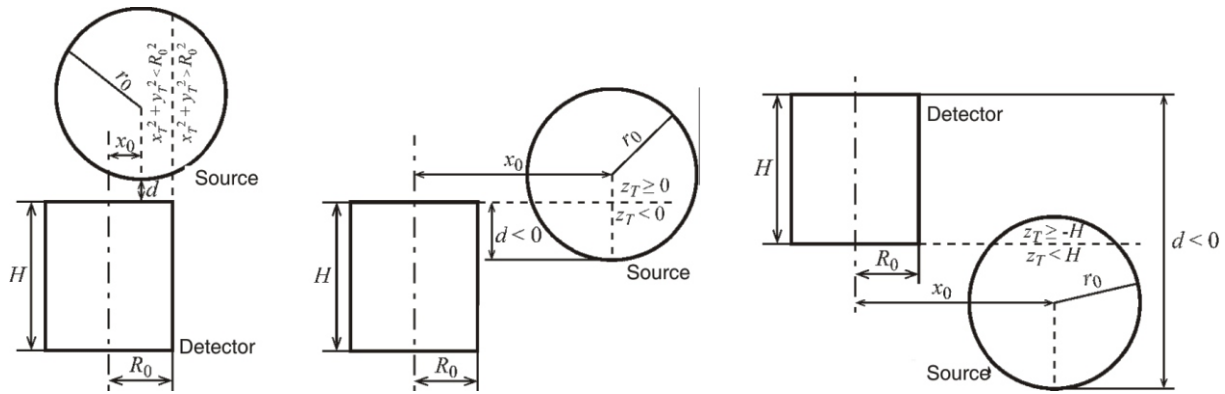


Figure 9. Various positions of a spherical source vs. the detector

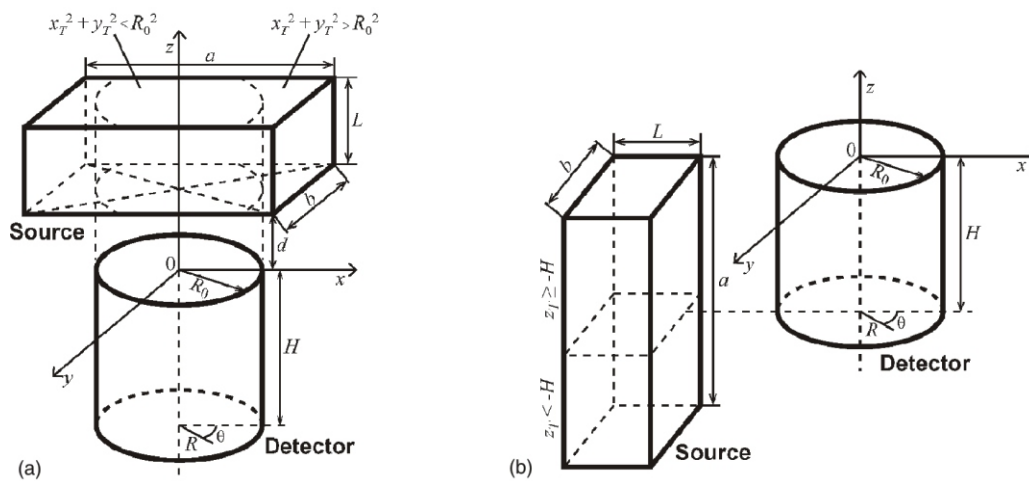


Figure 10. Cuboid source, two positions: coaxial (a) and by detector side (b)

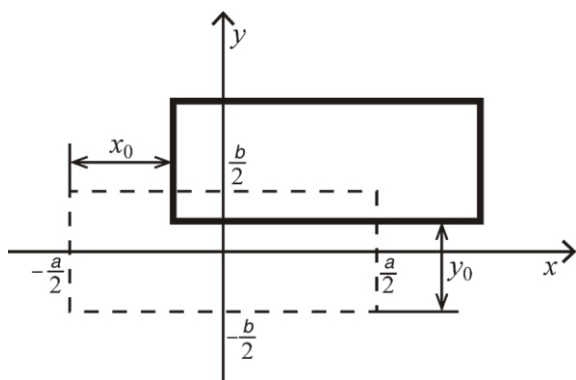


Figure 11. Horizontal axial displacement (in  $Oxy$  plane) of a cuboid source vs. the detector

### Computation times

Concerning the practical applicability, one should bear in mind the required computation times for efficiency calculations in the frameworks of particular tasks. In principle, computation times should be shorter (preferably much shorter) than counting times

for the actual samples – thus, not to be a limiting factor in laboratory practice. This can be taken as one of the acceptance criteria.

Although the steady speeding up of computers (thanks to ever more powerful hardware) is greatly helpful, optimization of numerical integration is still critical in this respect. In the current approach, optimization was strictly taken care of, enabling computation times to be kept at a reasonable/acceptable minimum. With modern personal computers it is a matter of minutes, even seconds – which is at least an order of magnitude shorter than times required for Monte Carlo – MC (*i. e.* statistical) calculations for the same calculation precision. Note that calculation precision is regulated either by segmentation of integration intervals (in numerical integration methods) or by the number of generated statistical events (in MC methods) – to the advantage of numerical integration.

In the advanced gamma spectrometry the previous fact transforms into the possibility of performing batch jobs of thousands of efficiency calculations, for the sake of deriving some *higher order* conclusions. A typical example is error propagation studying. For instance, in a study of the impact of detector crystal *bulletization* in gamma spectrometric analyses, more

than 150 000 efficiency calculations were prepared and performed in half a day time on an ordinary PC [21]. Such studies are apparently a key to the advanced gamma spectrometry.

The outlined mathematical model is intended to be gradually incorporated into ANGLE software, thus making it readily available for routine use by gamma spectrometry community. We believe this will be a significant step forward in advanced gamma spectrometry practice.

## NUMERICAL TESTING

In order to obtain an idea about the reliability and accuracy of the mathematical model – pending the appropriate experimental verification – we performed extensive numerical testing, as follows.

Mathematical models for some simpler, but widely used counting geometries (*e. g.* point, disc, cylinder and Marinelli sources, coaxially positioned with the detector) were developed a long time prior to the here described generalization. Extensive experimental verification and many years of successful practical application in numerous laboratories have confirmed both their reliability and accuracy (see *e. g.* ref. [18]). Comparing mathematical models for new geometries from the here elaborated generalized mathematical model with the previously verified ones, using numerical testing (simulation), is thus justified.

As an example, the mathematical model for efficiency calculations of rectangular cuboid (brick shape) sources was extensively numerically tested by comparing it to the previously/independently developed and well established/verified model of cylindrical sources. Results, as well as the methodology, are given in much detail in a separate paper [22]. Shortly, a brick shape source can be understood as a sort of interpolation between the corresponding outer and inner cylinders. By suitably varying dimensions and proportions of these, one can obtain a fair idea about the reliability (absence of systematic errors) and accuracy of the model. Also, by setting the source dimensions close to zero, it can be compared with previous models of disk shape and point sources. Finally, the introduction of the so called *equivoluminous* cylinder (having the same height and volume as the actual cuboid) gives another perspective to the comparison. The results obtained were exactly as expected, with effective solid angles (thus, detection efficiencies as well) for brick sources lying consistently, with no exception, between those of corresponding inner and outer cylinders, while reasonably close to equivoluminous cylinders. This clearly and conclusively indicates that the brick model is free of systematic errors (bugs), thus accurate and reliable.

We have performed a similar (although less extensive and differently structured) testing for a number

of practically applicable counting geometries. Results are affirmative and convincing as well, as illustrated in tabs. 1-4 for cylindrical, Marinelli, rectangular cuboid and spherical sources, respectively. Table 5 refers to testing various sources approaching zero dimensions (quasi point sources) by comparing the new results to those obtained by the previous approach (point sources). Realistic detector dimensions and counting configurations (source and its positioning *vs.* the detector) are used in all exercises; these are not presented in detail for the sake of conciseness. Here too, results are logically fitting into expected patterns of effective solid angle behavior/variations with varying geometrical parameters, favorably indicating the correctness of the mathematical model applied.

Despite the previously elaborated justification, it is well understood, of course, that numerical testing cannot replace experimental verification. Given the complexity of the latter, it is pending.

In tabs. 1 and 2,  $\overline{\Omega}$  denotes the effective solid angles calculated using the new mathematical model, while  $\overline{\Omega}_0$  is obtained by the appropriate previous model (relevant references are indicated). The  $\Delta$  [%] is the relative difference between the two, in %. All linear dimensions are in mm.

## PRACTICAL APPLICABILITY

It was the aim of the present work to enable practically unlimited applicability of gamma spectrometry in real situations. An extensive listing of the fields where gamma spectrometry is a method of either choice or back up would be too long, but some typical ones may include:

- environmental radioactivity monitoring,
- radiation protection,
- medicine and health physics,
- food safety,
- fuel cycle and nuclear industry,
- radioactive/nuclear waste management,
- regulatory control of radioactivity,
- radiological/nuclear emergency preparedness and response,
- geology and geochronology,
- metrology and nuclear data standardization,
- nuclear safety, security and safeguards,
- laboratory quality management,
- scientific research, and
- education and training, *etc.*

By resorting to the mathematical model presented, one can readily achieve practical solutions for a realistic gamma spectrometric case. It should be noted, nevertheless, that in practice a relatively small number of typical counting geometries (particularly cylindrical and Marinelli sources) account for the vast majority of measurements – the model may thus also serve to confirm the reliability of the existing models/software users are applying in their work.

**Table 1. Numerical testing of the new mathematical model for cylindrical sources, eq. (7), by comparison to previous models [15, 16]. Sources are positioned at the detector top, without and with axial displacement ( $x_0$ ); detector: HPGe coaxial**

$E_\gamma$	$r_0 < R_0, r_0 = 12 \text{ mm}, L = 25 \text{ mm}, \text{container wall} = 2 \text{ mm}, d = 6.1 \text{ mm}$						$r_0 > R_0, r_0 = 40 \text{ mm}, L = 55 \text{ mm}, \text{container wall} = 2.5 \text{ mm}, d = 6.6 \text{ mm}$					
	$x_0 = 0$			$x_0 = 9 \text{ mm}$			$x_0 = 0$			$x_0 = 9 \text{ mm}$		
	$\bar{\Omega}$	$\bar{\Omega}_0$	$\Delta [\%]$	$\bar{\Omega}$	$\bar{\Omega}_0$	$\Delta [\%]$	$\bar{\Omega}$	$\bar{\Omega}_0$	$\Delta [\%]$	$\bar{\Omega}$	$\bar{\Omega}_0$	$\Delta [\%]$
50	0.472647	0.472601	0.010	0.444023	0.444023	0.000	0.128098	0.127669	0.335	0.125396	0.125411	0.012
100	1.46302	1.46296	0.004	1.37421	1.37421	0.000	0.449401	0.448667	0.163	0.441442	0.441473	0.007
200	1.40720	1.40791	0.050	1.33018	1.33022	0.003	0.491352	0.491347	0.001	0.483383	0.483304	0.016
500	1.17998	1.18135	0.116	1.12239	1.12245	0.005	0.455746	0.457488	0.382	0.450172	0.449825	0.077
1000	1.02621	1.02772	0.147	0.979146	0.979208	0.006	0.418887	0.421502	0.624	0.414876	0.414393	0.116
3000	0.791933	0.793368	0.181	0.758291	0.758356	0.009	0.344715	0.347899	0.924	0.342564	0.341993	0.167
5000	0.743028	0.744415	0.187	0.711920	0.711984	0.009	0.328844	0.332058	0.977	0.327017	0.326441	0.176

**Table 2. Numerical testing of the new mathematical model for Marinelli sources, eq. (9), by comparison to the previous model [17]. Detectors: HPGe coaxial and LEPD**

$E_\gamma$	$r_0 = 60 \text{ mm}, L = 95 \text{ mm}, L_\varphi = 80 \text{ mm}, r_\varphi = 35 \text{ mm}, \text{container wall} = 2 \text{ mm}$						$r_0 = 60 \text{ mm}, L = 7 \text{ mm}, L_\varphi = 80 \text{ mm}, r_\varphi = 35 \text{ mm}, \text{container wall} = 2 \text{ mm}$					
	HPGe			LEPD			HPGe			LEPD		
	$\bar{\Omega}$	$\bar{\Omega}_0$	$\Delta [\%]$	$\bar{\Omega}$	$\bar{\Omega}_0$	$\Delta [\%]$	$\bar{\Omega}$	$\bar{\Omega}_0$	$\Delta [\%]$	$\bar{\Omega}$	$\bar{\Omega}_0$	$\Delta [\%]$
50	0.189844	0.190609	0.403	0.709919	0.711416	0.211	0.225634	0.225389	0.109	0.442804	0.442774	0.007
100	0.687228	0.691107	0.564	0.858830	0.863541	0.549	0.512806	0.510682	0.414	0.581143	0.581026	0.020
200	0.775072	0.779187	0.531	0.832765	0.837575	0.578	0.580243	0.573471	1.167	0.602005	0.601888	0.019
500	0.704583	0.709513	0.700	0.744796	0.748910	0.552	0.527377	0.520308	1.340	0.545788	0.545690	0.018
1000	0.633368	0.638516	0.813	0.669284	0.672872	0.536	0.471647	0.465155	1.376	0.490263	0.490167	0.020
3000	0.504865	0.509704	0.958	0.535025	0.537786	0.516	0.373183	0.368011	1.386	0.390917	0.390812	0.027
5000	0.477054	0.481741	0.982	0.505958	0.508536	0.510	0.351205	0.346316	1.392	0.368490	0.368383	0.029

**Table 3. Numerical testing of the new mathematical model for two cylindrical sources perpendicularly positioned vs. the detector axis, facing the detector side, eq. (8), by comparison to a rectangular cuboid source, eq. (11) [22],  $\bar{\Omega}_{RC}$  – rectangular cuboid,  $\bar{\Omega}_{LO}$  – laid out cylinder,  $\bar{\Omega}_{LI}$  – laid in cylinder,  $x_0 = 55 \text{ mm}, y_0 = 0$**

$E_\gamma$	$\bar{\Omega}_{LO}$	$\bar{\Omega}_{RC}$	$\bar{\Omega}_{LI}$	$\bar{\Omega}_{LO}$	$\bar{\Omega}_{RC}$	$\bar{\Omega}_{LI}$
	$r_0 = 12.5 \text{ mm}$ $L = 50 \text{ mm}$ $d = 42.9 \text{ mm}$	$a = 50 \text{ mm}$ $b = 25 \text{ mm}$ $L = 25 \text{ mm}$ $d = -42.9 \text{ mm}$	$r_0 = 17.7 \text{ mm}$ $L = 50 \text{ mm}$ $d = -48.1 \text{ mm}$	$r_0 = 35 \text{ mm}$ $L = 50 \text{ mm}$ $d = -65.9 \text{ mm}$	$a = 50 \text{ mm}$ $b = 70 \text{ mm}$ $L = 70 \text{ mm}$ $d = -65.9 \text{ mm}$	$r_0 = 50 \text{ mm}$ $L = 50 \text{ mm}$ $d = -80.9 \text{ mm}$
50	0.220336	0.216270	0.205603	0.162344	0.149261	0.131879
100	0.816689	0.800290	0.761793	0.596558	0.548907	0.468995
200	0.896052	0.879185	0.840975	0.670642	0.621660	0.535789
500	0.793455	0.780456	0.751725	0.612430	0.571243	0.496910
1000	0.703761	0.693366	0.670801	0.553336	0.517886	0.453094
3000	0.552762	0.545688	0.530719	0.444211	0.417402	0.367752
5000	0.520762	0.514397	0.501060	0.420979	0.395965	0.349524

In facilitating the previous, providing adequate computer codes is apparently crucial. A gradual introduction of the mathematical model into ANGLE software [18] is therefore highly desirable.

### CONCLUSION

In the present paper, a generalized formula for the calculation of effective solid angles is elaborated,

with the aim of paving the way and clearing the limitations to quantification of gamma spectroscopic measurements (*i. e.* gamma spectrometry) in practical conditions. Semi empirical efficiency transfer approach is employed, while efficiencies are calculated using the effective solid angle concept. Generalization is achieved through unlimited flexibility, yet simplicity in organizing/structuring numerical integration intervals. Crucially, integration limits over the source do not depend on the detector whatsoever. The examples

**Table 4. Numerical testing of the new mathematical model for a spherical source  $\bar{\Omega}_S$ , eq. (10), by comparison to the equivoluminous cylindrical source  $\bar{\Omega}_C$ , eq.(7), without and with axial displacement ( $x_0$ ); various positions vs. the detector (d) are considered**

$E_\gamma$	$\bar{\Omega}_S$	$\bar{\Omega}_C$	$\bar{\Omega}_S$	$\bar{\Omega}_C$	$\bar{\Omega}_S$	$\bar{\Omega}_C$	$\bar{\Omega}_S$	$\bar{\Omega}_C$
	$x_0 = 0$ $d = 4.1$ mm	$x_0 = 0$ $d = 6.628$ mm	$x_0 = 12$ mm $d = 4.1$ mm	$x_0 = 12$ mm $d = 6.628$ mm	$x_0 = 50$ mm $d = -20.9$ mm	$x_0 = 50$ mm $d = -18.372$ mm	$x_0 = 50$ mm $d = -80.9$ mm	$x_0 = 50$ mm $d = -78.372$ mm
50	0.322976	0.330157	0.281971	0.285538	0.137715	0.141256	0.182847	0.191010
100	1.00465	1.03903	0.896567	0.920019	0.564322	0.575498	0.567284	0.577581
200	1.00609	1.04127	0.914182	0.940302	0.665290	0.674070	0.649138	0.655709
500	0.868444	0.896866	0.799348	0.821247	0.620362	0.625237	0.602586	0.605582
1000	0.766949	0.790852	0.710360	0.729129	0.564203	0.567096	0.547456	0.548778
3000	0.602791	0.620461	0.562296	0.576522	0.455778	0.456741	0.441965	0.441790
5000	0.567814	0.584207	0.530372	0.543632	0.431466	0.432058	0.418378	0.417928

**Table 5. Numerical testing of the new mathematical model for various source shapes, by converging source dimensions to zero (quasi-point sources); results given for coaxial positioning ( $x_0 = 0, y_0 = 0$ ) and with axial displacement; the indices denote: CC – coaxial cylinder, CP – perpendicular cylinder, RC – rectangular cuboid, S – sphere, P – point; source dimensions are  $r_0 = L = a = b = 0.001$  mm**

$E_\gamma$	$\bar{\Omega}_{CC}$	$\bar{\Omega}_{CP}$	$\bar{\Omega}_{RC}$	$\bar{\Omega}_S$	$\bar{\Omega}_P$
	$x_0 = 0$	$x_0 = 0$	$x_0 = 0$ $y_0 = 0$	$x_0 = 0$ $y_0 = 0$	$x_0 = 0$
50	0.592766	0.592752	0.592767	0.592752	0.592627
100	1.65497	1.65492	1.65497	1.65492	1.65470
200	1.53230	1.53226	1.53230	1.53226	1.53206
500	1.23005	1.23002	1.23005	1.23002	1.229901
1000	1.03930	1.03927	1.03930	1.03927	1.03921
3000	0.775281	0.775262	0.775282	0.775262	0.775249
5000	0.719431	0.719413	0.719431	0.719413	0.719411
	$x_0 = 60$ mm	$x_0 = 60$ mm	$x_0 = 60$ mm $y_0 = 0$	$x_0 = 60$ mm $y_0 = 0$	$x_0 = 60$ mm
50	0.069433	0.069433	0.069434	0.069433	0.068843
100	0.35389	0.353888	0.353891	0.353886	0.351894
200	0.411535	0.411514	0.411485	0.411502	0.409954
500	0.365642	0.365584	0.365511	0.365558	0.365171
1000	0.321919	0.321848	0.321774	0.321821	0.321876
3000	0.25014	0.250062	0.249989	0.250035	0.250549
5000	0.233872	0.233793	0.23372	0.233766	0.234393
	$x_0 = 0$ $y_0 = 60$ mm	$x_0 = 0$ $y_0 = 60$ mm	$x_0 = 30$ mm $y_0 = 51.96$	$x_0 = 30$ mm $y_0 = 51.96$	$x_0 = 60$ mm
50	0.069446	0.069447	0.06942	0.069421	0.068843
100	0.354011	0.354015	0.353941	0.353945	0.351894
200	0.411588	0.411577	0.411499	0.411517	0.409954
500	0.365623	0.365583	0.36555	0.365584	0.365171
1000	0.321875	0.32183	0.321817	0.32185	0.321876
3000	0.250079	0.25003	0.250035	0.250067	0.250549
5000	0.233808	0.233759	0.233767	0.233799	0.234393

elaborated prove practical applicability in a straightforward manner, while numerical testing confirms its reliability.

Despite complex calculations (high precision five-fold numerical integration), computation times are kept within order of minutes (or less). This enables

creation of batch jobs and computation of numerous (thousands, even millions) efficiency values in short periods of time, from which higher-level conclusions can be derived – facilitating the practice of advanced gamma spectrometry likewise.

## AUTHORS' CONTRIBUTIONS

N. N. Mihaljević developed the mathematical model presented in the paper, sublimating 30 years of work on the topic, and also performed the numerical testing. A. D. Dlabac is devoted to ANGLE software development, consistently adding the value by transforming/embodying theoretical results of the group into user-oriented tool and made a valuable contribution in various phases of the work. S. I. Jovanović conceived and guided the research and wrote the paper. All authors extensively interacted, exchanging the ideas, in particular during the preparation of the manuscript.

## REFERENCES

- [1] Debertin, K. R, Helmer G., Gamma and X ray Spectrometry with Semiconductor Detectors, North Holland, New York, USA, 1988
- [2] Knoll, G. F, Radiation Detection and Measurement, 3<sup>rd</sup> Edition, John Wiley & Sons, New York, USA, 2000
- [3] Gilmore, G. R, Practical Gamma ray Spectrometry, 2<sup>nd</sup> Edition, John Wiley & Sons, New York, USA, 2008
- [4] Jovanović, S., et al., ANGLE: A PC Code for Semiconductor Detector Efficiency Calculations, *J. Radioanal. Nucl. Chem.*, 218 (1997), 1, pp. 13-20
- [5] Moens, L., et al., Calculation of the Absolute Peak Efficiency of Gamma Ray Detectors for Different Counting Geometries, *Nucl. Instrum. Methods Phys. Res.*, 187 (1981), 2-3, pp. 451-472
- [6] Jovanović, S., et al., ANGLE v2.1 – New Version of the Computer Code for Semiconductor Detector Gamma Efficiency Calculations, *Nucl. Instrum. Methods Phys. Res. A*, 622 (2010), 2, pp. 385-391
- [7] Sima, O., Arnold, D., Transfer of the Efficiency Calibration of Germanium gamma Ray Detectors Using the GESPECOR Software, *Appl. Rad. Isot.*, 56 (2002), 1-2, pp. 71-75
- [8] Piton, F., et al., Efficiency Transfer and Coincidence Summing Corrections for  $\gamma$ -ray Spectrometry, *Appl. Radiat. Isot.*, 52 (2000), 3, pp. 791-795
- [9] Lepy, M. C., et al., Intercomparison of Efficiency Transfer Software for Gamma Ray Spectrometry, *Appl. Radiat. Isot.*, 55 (2001), 4, pp. 493-503
- [10] Vidmar, T., et al., Testing Efficiency Transfer Codes for Equivalence, *Appl. Radiat. Isot.*, 68 (2010), 2, pp. 355-359
- [11] Moens, L., et al., Calculation of the Absolute Peak Efficiency of Ge and Ge(Li) Detectors for Different Counting Geometries, *J. Radioanal. Chem.*, 70 (1982), 1-2, pp. 539-550
- [12] Erten, H. N., et al., H., Efficiency Calibration and Summation Effects in Gamma Ray Spectrometry, *J. Radioanal. Nucl. Chem.*, 125 (1988), 1, pp. 3-10
- [13] Vidmar, T., Likar, A., On the Invariability of the Total to Peak Ratio in Gamma Ray Spectrometry, *Appl. Radiat. Isot.*, 60 (2004), 2-4, pp. 191-195
- [14] Jovanović, S., et al., The Effective Solid Angle Concept and ANGLE v3.0 Computer Code for semiconductor Detector Gamma Efficiency Calculations – Applicability to *In Situ* Characterization of Contaminated Sites, IAEA Analytical Quality in Nuclear Applications Series No. 49: *In Situ* Analytical Characterization of Contaminated Sites Using Nuclear Spectrometry Techniques Review of Methodologies and Measurements, Vienna, Austria, 2017, pp. 141-158
- [15] Vukotić, P., et al., On the Applicability of the Effective Solid Angle Concept in Activity Determination of large Cylindrical Sources, *J. Radioanal. Nucl. Chem.*, 218 (1997), 1, pp. 21-26
- [16] Mihaljević, N., et al., EXTSANGLE – an Extension of the Efficiency Conversion Program SOLANG to Sources with a Diameter Larger than that of the Ge Detector, *J. Radioanal. Nucl. Chem.*, 169 (1993), pp. 209-215
- [17] Mihaljević, N., et al., Calculation of Full Energy Peak Detection Efficiencies of Semiconductor Detectors for Some Interesting Counting Geometries, Proc. of the Intern. k0 Users Workshop (30 Sept.-2 Oct. 1992), Gent, Astene, Belgium, pp. 53-57  
[http://www.kayzero.com/k0naa/k0naaorg/k0-Users\\_Workshops/Entries/1992/9/30\\_Gent\\_Belgium\\_files/Workshop%20Proceedings%201992.pdf](http://www.kayzero.com/k0naa/k0naaorg/k0-Users_Workshops/Entries/1992/9/30_Gent_Belgium_files/Workshop%20Proceedings%201992.pdf)
- [18] \*\*\*, ANGLE 4 – Advanced Gamma Spectrometry Software, <https://www.angle4.com>
- [19] Abas, M. I. et al., Full Energy Peak Efficiency of Asymmetrical Polyhedron Germanium Detector, *Nucl Technol Radiat*, 33 (2018), 2, pp. 150-158
- [20] Mihaljević, N., et al., Accounting for Detector Crystal Edge Rounding (Bulletization) in Gamma Efficiency Calculations – Theoretical Elaboration and Practical Application in ANGLE software, *Nucl. Technol. Radiat*, 27 (2012), 1, pp. 1-12
- [21] Dlabac, A., Numerical Results of the Study on the Effect of Bulletization on HPGe Detector Gamma Efficiency Calculations, [www.angle.dlabac.com/bulletization\\_study.html](http://www.angle.dlabac.com/bulletization_study.html)
- [22] Mihaljević, N., et al., A Mathematical Model of Semiconductor Detector Gamma Efficiency Calibration for rectangular Cuboid (Brick Shape) Sources, *Nucl Technol Radiat*, 33 (2018), 2, pp. 139-149

Received on October 31, 2018

Accepted on February 2, 2019

Никола Н. МИХАЉЕВИЋ, Слободан И. ЈОВАНОВИЋ, Александар Д. ДЛАБАЧ

**ГЕНЕРАЛИЗОВАНИ МАТЕМАТИЧКИ МОДЕЛ ЗА  
КАЛИБРАЦИЈУ ЕФИКАСНОСТИ ДЕТЕКТОРА ГАМА-ЗРАЧЕЊА  
Примена у реалним случајевима**

Калибрација ефикасности, тј. одређивање ефикасности детекције ( $\epsilon_p$ ), кључно је питање у гама-спектрометрији (квантификацији гама-спектроскопских мерења) помоћу полупроводничких и сцинтилационих детектора. Поређењем три приступа – релативног, апсолутног и полумпиријског – закључено је да полумпиријски има значајне предности. У том смислу издвојен је и описан принцип “трансфера ефикасности” помоћу ефективних просторних углова ( $\bar{\Omega}$ ). Овим приступом се проблем калибрације ефикасности своди на одређивање  $\bar{\Omega}$ , што је већ уобичајена пракса у гама спектрометрији, углавном кроз коришћење софтвера ANGLE. Потом је дата генерализована математичка формула (прва те врсте) за прорачун  $\bar{\Omega}$ , чиме се отвара могућност за напредне примене гама-спектрометрије. Формула пружа неограничену флексибилност у примени, јер раздваја извор и детектор у процесу интеграљења (прорачун  $\bar{\Omega}$ ). Њена практична применљивост показана је на неколико типичних примера који се сусрећу у реалним ситуацијама гама-мерења, као и у неким неубичајеним случајевима. Формуле за ове конкретне случајеве су онда коришћене за нумеричку проверу на РС рачунару. Приликом рада посебно је вођено рачуна о оптимизацији комплексних нумеричких процедура (које укључују петоструку нумеричку интеграцију), да би се време потребно за прорачун svelo на најмању могућу меру (ред величине неколико минута на просечном РС рачунару). Добијени резултати потврђују исправност поменутих формула и пратећег софтвера. Модел ће се поступно уграђивати у софтвер ANGLE, чиме ће бити стављен на располагање гама-спектрометријској заједници.

*Кључне речи: гама-спектрометрија, ефикасности детекције, калибрација детектора, математички модел, нумеричка провера, применљивости, ANGLE софтвер*

---